Electronic Supplementary Material (ESI) for Journal of Materials Chemistry A.

Supporting Information

Achieving high energy storage in $BaTiO_3$/rGO/PVDF nanocomposites by regulating the charge transfer path at the hetero-interface

Yange Yu, Wenzhu Shao, Yue Liu, Yang Li, Jing Zhong, Huijian Ye, Liang Zhen**

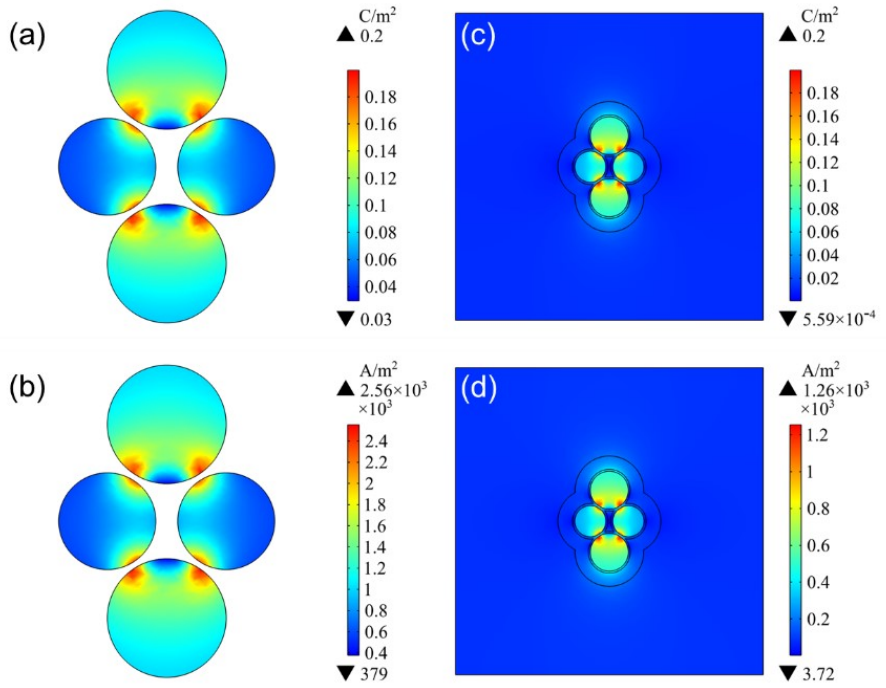

Figure S1. The simulated results of BTO/PVDF nanocomposite: (a) the polarization and (b) current density of BTO NPs, (c) the polarization and (d) current density of BTO NPs in PVDF matrix.

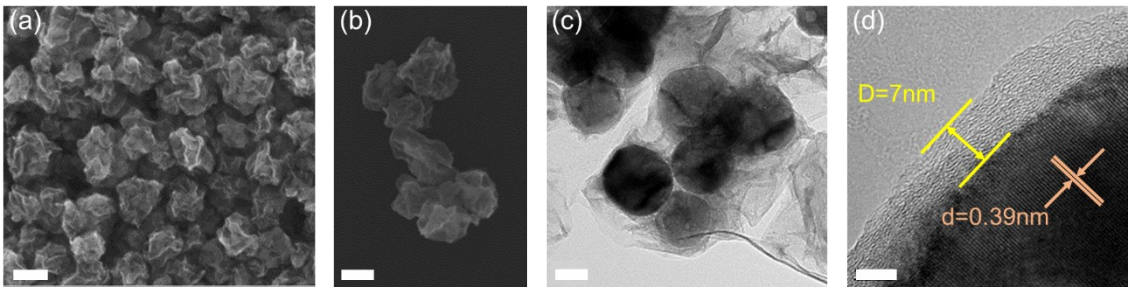

Figure S2. (a, b) SEM images of BTO@rGO NPs, scale bar: 200nm; (c) TEM image, sacle bar: 50nm; (d) HRTEM image, scale bar: 5nm.

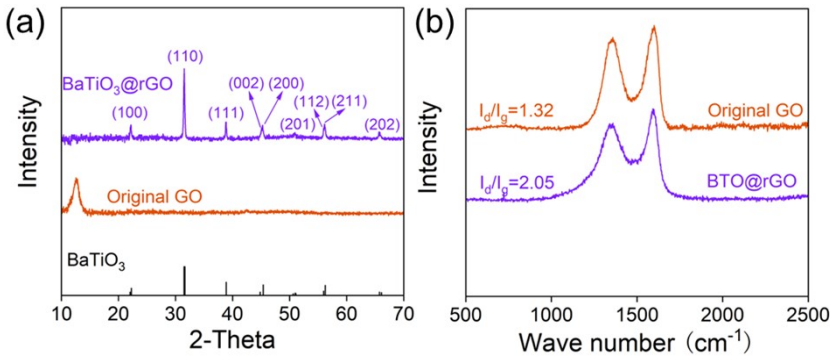

Figure S3. (a) XRD patterns, (b) Raman spectra of GO nanosheets and BTO@rGO NPs.

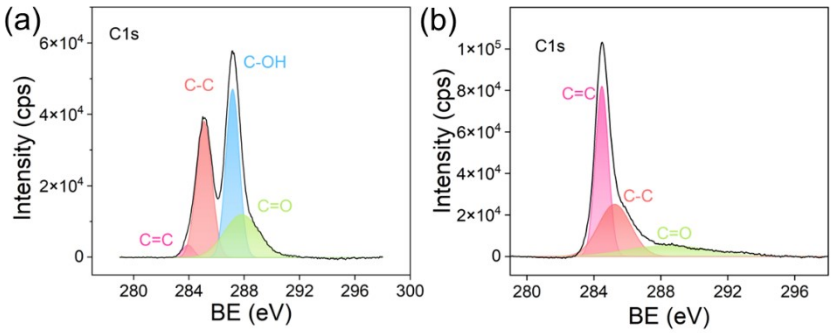

Figure S4. Typical high-resolution XPS spectra of C1s region of (a) GO nanosheets, (b) BTO@rGO NPs.

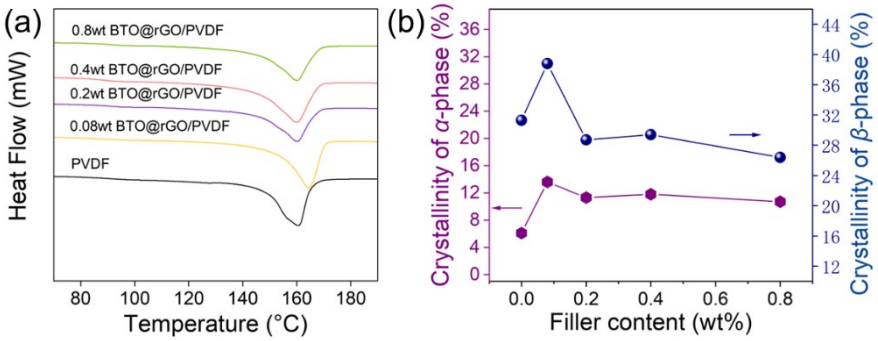

Figure S5. (a) DSC cruves of BTO@rGO/PVDF nanocomposites, (b) Comparation of crystallinity of α-phase and β-phase.

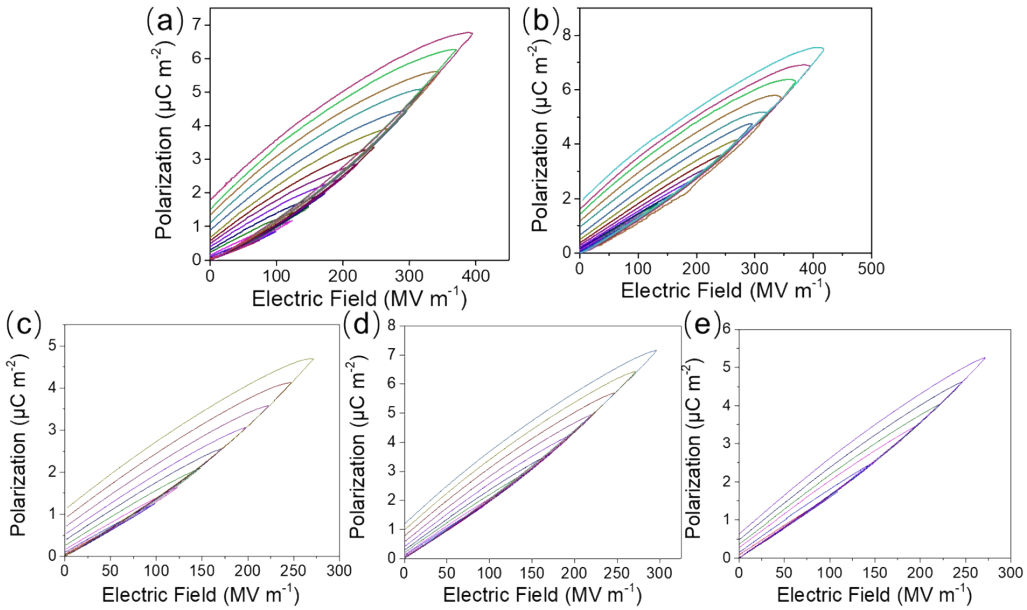

Figure S6. D-E loops of the BTO@rGO/PVDF nanocomposites with various loadings measured under different electric fields. (a) PVDF, (b) 0.08wt%, (c) 0.2wt%, (d) 0.4wt%, (e) 0.8wt%.

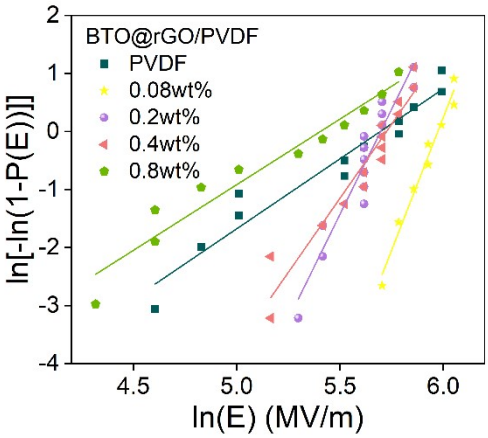

Figure S7. The Weibull distribution of BTO@rGO/PVDF nanocomposites.

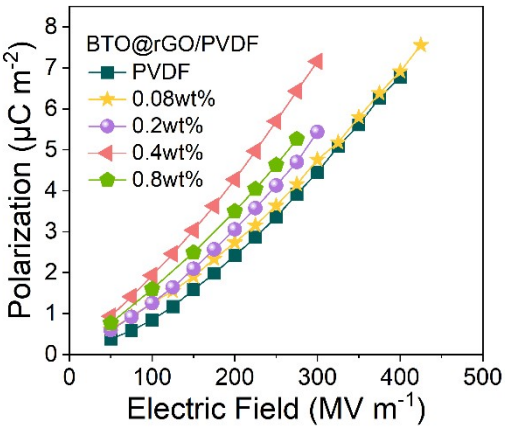

Figure S8. The polarization of BTO@rGO/PVDF nanocomposite with filler content varies.

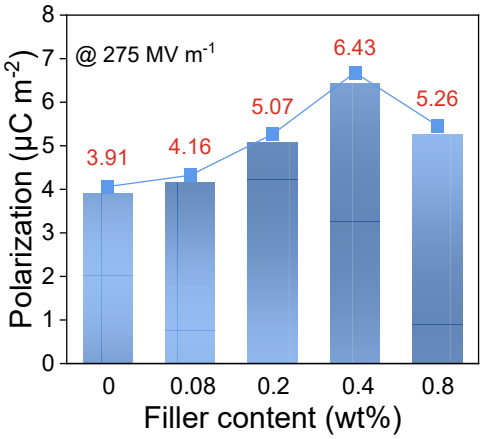

Figure S9. Polarization of BTO@rGO/PVDF nanocomposites varies by electric field and filler content.

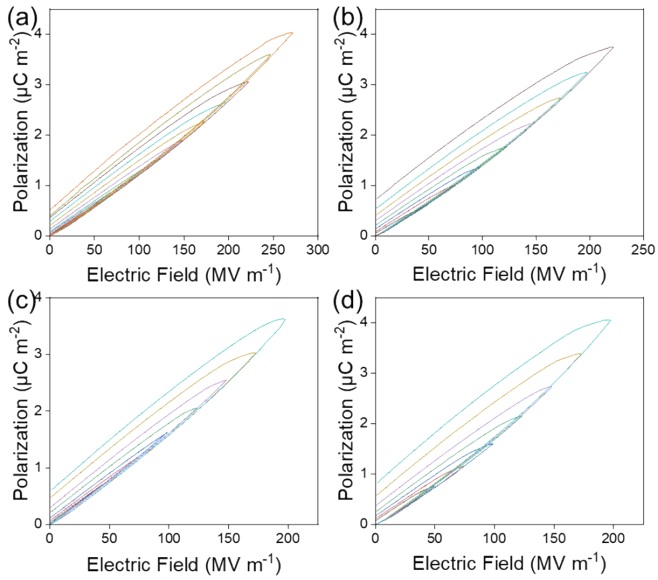

Figure S10. D-E loops of the BTO/PVDF nanocomposites with various loadings measured under different electric fields. (a) 0.08wt%, (b) 0.2wt%, (c) 0.4wt%, (d) 0.8wt%.

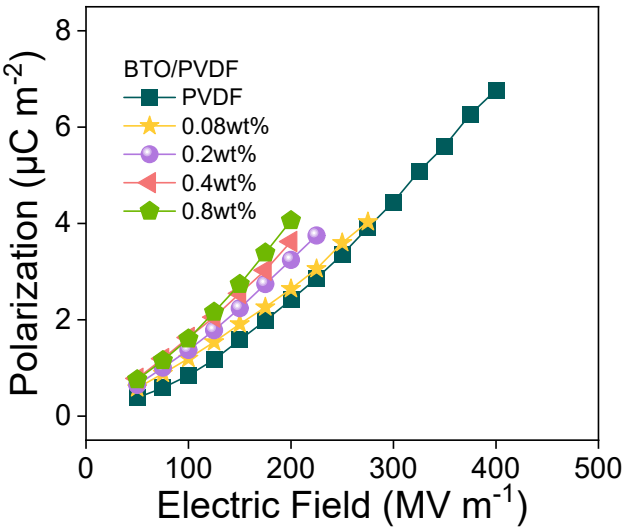

Figure S11. Polarization of BTO/PVDF nanocomposites varies by electric field with various filler contents.

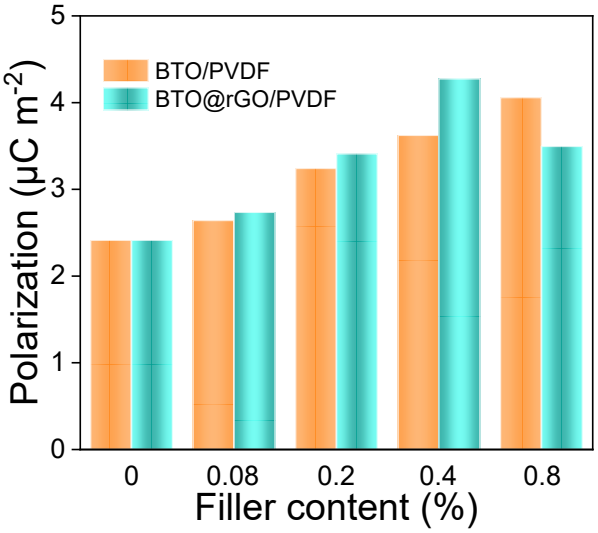

Figure S12. Comparison of polarization between BTO/PVDF and BTO@rGO/PVDF at 200 MV m^{-1}.

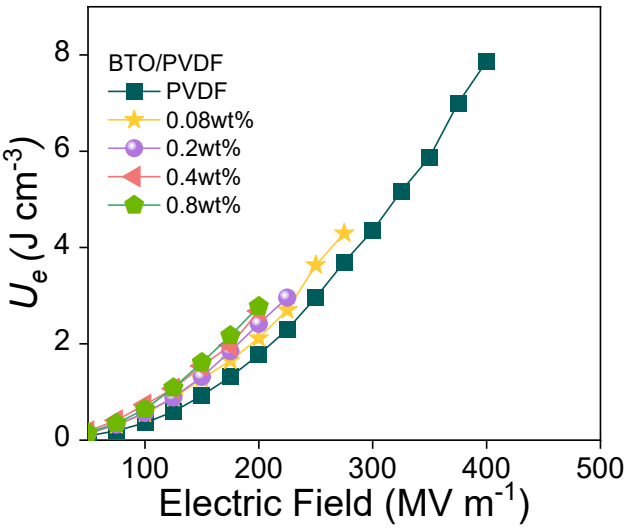

Figure S13. Polarization of BTO/PVDF nanocomposites varies by electric field with various filler contents.

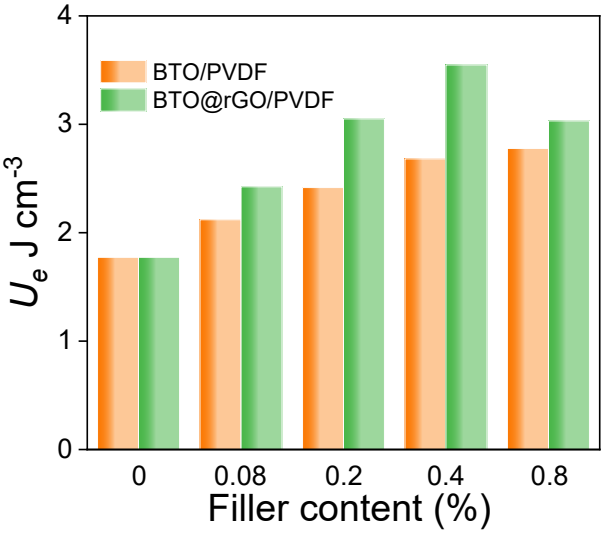

Figure S14. Comparison of U_e between BTO/PVDF and BTO@rGO/PVDF at 200 MV m^{-1}.

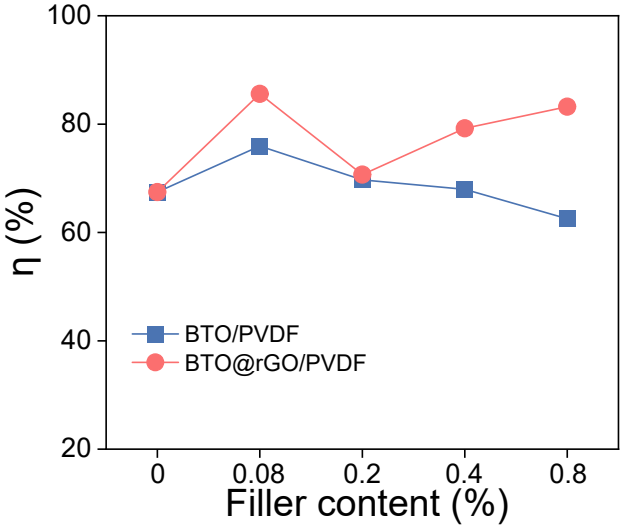

Figure S15. Comparison of η between BTO/PVDF and BTO@rGO/PVDF at 200 MV m^{-1}.

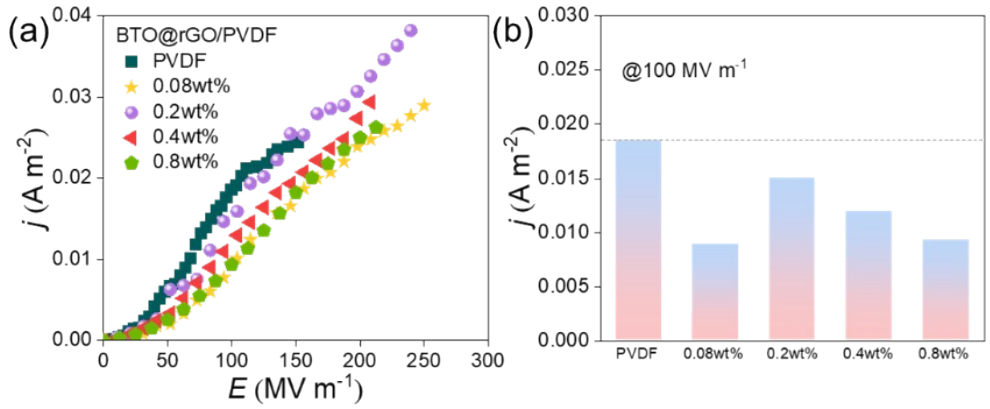

Figure S16. (a) *j–E* curves of BTO@rGO/PVDF nanocomposites filled with various content of BTO@rGO nanoparticles (b) Variation of current density PVDF-based nanocomposite filled with various content of BTO@rGO NPs at 100 MV m^{-1}.

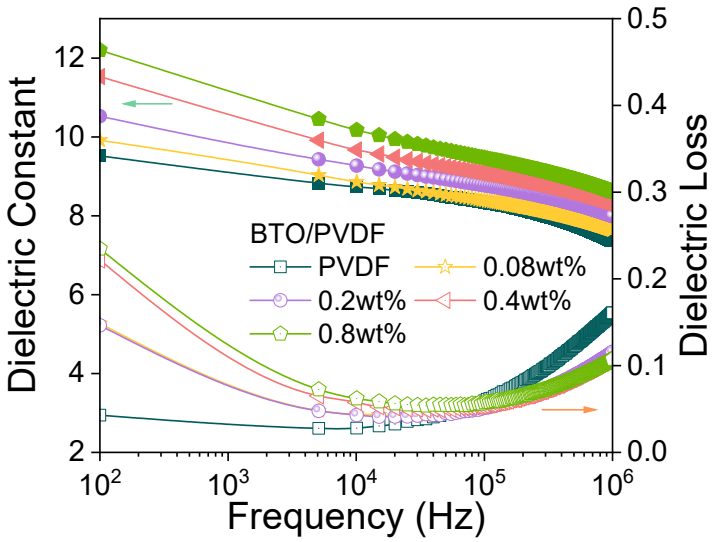

Figure S17. The frequency-dependence dielectric constant and dielectric loss of BTO/PVDF nanocomposites.

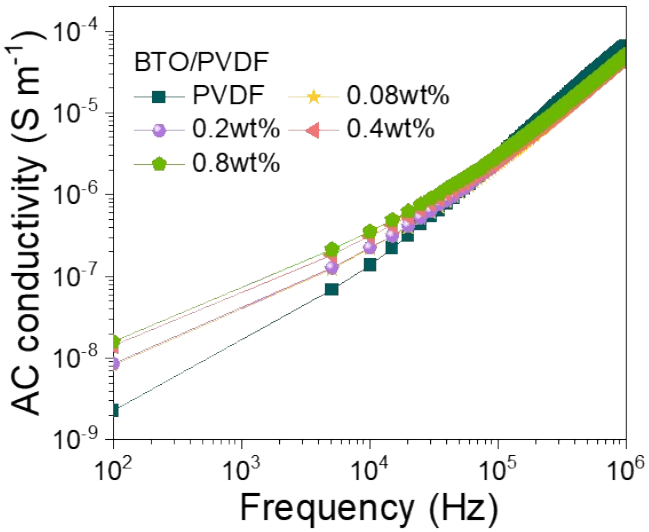

Figure S18. The frequency-dependent AC conductivity of BTO/PVDF nanocomposites.

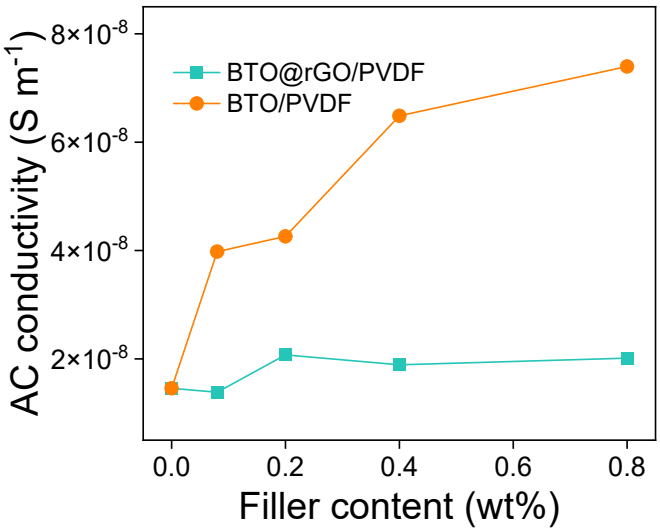

Figure S19. Comparision of AC conductivity versus BTO/PVDF and BTO@rGO/PVDF nanocomposites at 1kHz.

Table S1. The content of β-phase varies with the contention of BTO@rGO nanoparticles

Samples	$F(\beta)$	$F(\alpha)$
	K_β=7.7 × 10^4	K_α=6.1 × 10^4
PVDF	83.7%	16.3%
0.08wt% BTO@rGO/PVDF	74.1%	25.9%
0.2wt% BTO@rGO/PVDF	71.7%	28.3%
0.4wt% BTO@rGO/PVDF	71.4%	28.6%
0.8wt% BTO@rGO/PVDF	71.3%	28.7%

Table S2. The crystallity of α-phase and β-phase varies with the contention of BTO@rGO NPs

Samples	X_c	X_α	X_β
PVDF	37.4%	6.1%	31.3%
0.08wt% BTO@rGO/PVDF	52.4%	13.6%	38.8%
0.2wt% BTO@rGO/PVDF	40.0%	11.3%	28.7%
0.4wt% BTO@rGO/PVDF	41.2%	11.8%	29.4%
0.8wt% BTO@rGO/PVDF	37.1%	10.7%	26.4%

Note 1 The calculation of the content of *β*-phase and α-phase based on FTIR.

The A_α absorbance at 766 $cm^{-1}$and A_β absorbance at 840 cm^{-1} are given by the following equations under the assumption that IR absorption follows the Lambert-Beer law:

$$A_\alpha = log\frac{I_\alpha^0}{I_\alpha} = K_\alpha C X_\alpha h \quad (1)$$

$$A_\beta = log\frac{I_\beta^0}{I_\beta} = K_\beta C X_\beta h \quad (2)$$

$$F(\beta) = \frac{X_\beta}{X_\alpha + X_\beta} = \frac{A_\beta}{(K_\beta/K_\alpha)A_\alpha + A_\beta} \quad (3)$$

where h is the thickness of samples; and C represents the average total monomer concentration, which is a constant. The incident and transmitted intensity radiations were denoted by I^0 and I respectively. The subscript represents the type of crystalline phase. The X with subscript represents the crystallinity of the specified phase. The values of K_α and K_β were 6.1×10^4 and 7.7×10^4 cm^2 mol^{-1} respectively, which respect the absorption coefficient at the respective wavenumber.

Note 2 Finite Element Method (FEM) Modeling

To explore the effect of the rGO layer on the polarization and current density in the PVDF matrix, the numerical simulation was performed by finite element method (FEM).and AC/DC module of COMSOL software. The model size was 0.8 μm × 0.8 μm, the core (BTO) diameter was 80 nm, the shell (rGO) thickness was 5nm, and the transition zone thickness was 35nm. The periodic model of a single particle is analyzed by using a unitized extensible periodic model. The governing equation in the COMSOL model is:

$$\nabla \cdot (D) = \rho \quad (5)$$

$$\nabla \cdot j = \frac{-\partial \rho}{\partial t} \quad (5)$$

$$D = \varepsilon_0 \varepsilon_r E \quad (6)$$

$$E = -\nabla\varphi \tag{7}$$

where σ is the conductivity of the material, j is Current density, E is electric field, D is the electric displacement vector, ε_0 represents the vacuum dielectric constant, ε_r represents the relative dielectric constant, ρ represents the density of space charge.

The electrical nonlinearity of rGO and PVDF under ultra-high pressure can be described by Poole-Frenkel effect, then the conductance is corrected

$$\sigma_c = \sigma_0 exp[\frac{\sqrt{e^3 E/\pi\varepsilon_0\varepsilon_r}}{kT}] , \tag{8}$$

where σ_0 is the original conductance, e is the electron charge, T is the thermodynamic temperature, ε_r is relative dielectric constant and k is Boltzman constant.

Apply a 150 MV m^{-1} electric field vertically from the top to the bottom of the model while setting the bottom to the ground. The relative dielectric constant of rGO and PVDF is respectively set as 18 and 10. The original conductance of rGO and PVDF is set as 2.68 S m^{-1} and 1×10^{-15} S/m. The relative dielectric constant and conductance of BTO are set as 1400 and 1×10^{-5} S/m. The polarization and current density of BTO/PVDF and BTO@rGO/PVDF nanocomposites were simulated in a three-dimensional model and the results of two-dimensional section are as shown in Fig. 1 and Fig. S1.

The FEM-based software of COMSOL version 6.0 is used for solving differential equations. The MUMPS solver and BiCGStab solver are used to completing the iteration process.